Journal of Hazardous Materials 383 (2020) 121153

Contents lists available at ScienceDirect

Journal of Hazardous Materials

journal homepage: www.elsevier.com/locate/jhazmat

Antimicrobial efficacy and mechanisms of silver nanoparticles against *Phanerochaete chrysosporium* in the presence of common electrolytes and humic acid

Zhenzhen Huang[a,1], Zhuotong Zeng[b,1], Zhongxian Song[c,1], Anwei Chen[d,1], Guangming Zeng[a,*], Rong Xiao[b,*], Kai He[a], Lei Yuan[a], Hui Li[a], Guiqiu Chen[a]

[a] College of Environmental Science and Engineering, Hunan University and Key Laboratory of Environmental Biology and Pollution Control (Hunan University), Ministry of Education, Changsha 410082, China
[b] Department of Dermatology, Second Xiangya Hospital, Central South University, Changsha 410011, China
[c] Faculty of Environmental and Municipal Engineering, Henan Key Laboratory of Water Pollution Control and Rehabilitation Technology, Henan University of Urban Construction, Pingdingshan 467036, China
[d] College of Resources and Environment, Hunan Agricultural University, Changsha 410128, China

GRAPHICAL ABSTRACT

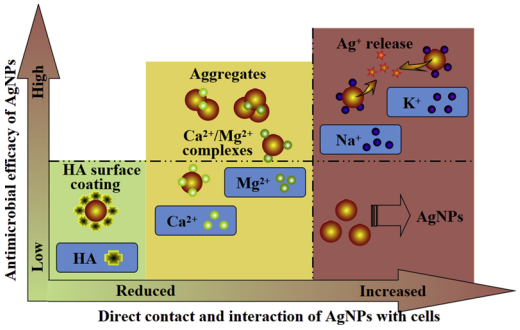

ARTICLE INFO

Editor: Daniel C.W. Tsang

Keywords:
Silver nanoparticles
Antimicrobial efficacy
Phanerochaete chrysosprium
Monovalent and divalent electrolytes
Humic acid

ABSTRACT

In this study, influences of cations (Na^+, K^+, Ca^{2+}, and Mg^{2+}), anions (NO_3^-, Cl^-, and SO_4^{2-}), and humic acid (HA) on the antimicrobial efficacy of silver nanoparticles (AgNPs)/Ag^+ against *Phanerochaete chrysosporium* were investigated by observing cell viability and total Ag uptake. K^+ enhanced the antimicrobial toxicity of AgNPs on *P. chrysosporium*, while divalent cations decreased the toxicity considerably, with preference of Ca^{2+} over Mg^{2+}. Impact caused by a combination of monovalent and divalent electrolytes was mainly controlled by divalent cations. Compared to AgNPs, however, Ag^+ with the same total Ag content exhibited stronger antimicrobial efficacy towards *P. chrysosporium*, regardless of the type of electrolytes. Furthermore, HA addition induced greater microbial activity under AgNP stress, possibly originating from stronger affinity of AgNPs over Ag^+ to organic matters. The obtained results suggested that antimicrobial efficacy of AgNPs was closely related to water chemistry: addition of divalent electrolytes and HA reduced the opportunities directly for AgNP contact and interaction with cells through formation of aggregates, complexes, and surface coatings, leading to sig-

* Corresponding authors.
E-mail addresses: zgming@hnu.edu.cn (G. Zeng), xiaorong65@csu.edu.cn (R. Xiao).
[1] Zhenzhen Huang, Zhuotong Zeng, Zhongxian Song and Anwei Chen contributed equally to this article.

https://doi.org/10.1016/j.jhazmat.2019.121153
Received 11 April 2019; Received in revised form 2 September 2019; Accepted 3 September 2019
Available online 04 September 2019
0304-3894/

nificant toxicity reduction; however, in monovalent electrolytes, the dominating mode of action of AgNPs could be toxic effects of the released Ag^+ on microorganisms due to nanoparticle dissolution.

1. Introduction

Silver nanoparticles (AgNPs), one of the most extensively studied nanomaterials, are increasingly used in consumer products including paints, textiles, medicals, personal care products, and food storage bins (Chambers et al., 2014; Levard et al., 2012; He et al., 2017; Gong et al., 2009), due to their broad-spectrum antimicrobial efficacy and low mammalian cytotoxicity (Huang et al., 2016; Li and Lenhart, 2012; Zhang et al., 2015). Increased AgNP production and usage imply an increase potential for their release into surface waters and subsurface, thus transforming into various silver forms (e.g., Ag^0 nanoparticle, dissolved Ag^+, and soluble AgNP/Ag^+ complexes) due to the oxidation and dissolution of nanoparticles (Liu and Hurt, 2010; Guo et al., 2017; Xiu et al., 2012; Zuo et al., 2015). The incidental or intentional release of AgNPs to the environment poses a potential risk to the ecosystem and human health (Tan et al., 2015; Deng et al., 2013; Chen et al., 2015a; Zhang et al., 2019; Zhou et al., 2018; He et al., 2019; Zhou et al., 2019). The toxicity and antimicrobial activity of AgNPs are proven to be associated with water chemistry, which shows impacts on aggregation, dissolution, and stability of AgNPs (Li et al., 2011a; Jin et al., 2010; Long et al., 2011; Tejamaya et al., 2012; Deonarine et al., 2011).

For example, divalent cations (e.g., Ca^{2+} and Mg^{2+}) were more efficient in AgNP aggregation and conferred protective effects against cytotoxicity of nanoparticles via potentially limiting their adherence onto microbial biomass as compared to monovalent cations (e.g., Na^+) at similar concentrations (Anderson et al., 2014; Zhang and Oyanedel-Craver, 2012). Nevertheless, Pokhrel et al. (2014a) exhibited an enhanced toxicity of AgNPs with increasing Ca^{2+} concentrations. Besides, effects of aqueous anions on AgNP stability behaviors have also been reported (Guo et al., 2017; Xiu et al., 2011). Chloride strongly enhanced the destabilization of AgNPs through the formation of $AgCl^0$ bridging of AgNPs, respectively (Chambers et al., 2014; Tejamaya et al., 2012). Association of these anions with released Ag^+ may form precipitates or soluble complexes (Li et al., 2010; Liang et al., 2017). These behaviors would further reduce AgNP/Ag^+ bioavailability and toxicity. By contrast, AgNP stability was increased in the presence of phosphate and bicarbonate (Afshinnia and Baalousha, 2017). However, no specific ion effects were observed for nitrate (NO_3^-) and sulfate (SO_4^{2-}) as described by Baalousha et al. (2013). Moreover, natural organic material (NOM) could enhance AgNP stability through steric or electrostatic repulsion after being adsorbed onto nanoparticle surface, playing an important role in the environmental fate, transport, and toxicity of nanomaterials (Liu et al., 2014; Wagner et al., 2014; SharMa et al., 2014; Zhang et al., 2006). Enhanced aggregation was also documented in certain systems when NOM was complexed with cations and intermolecular bridging of humic acid (HA) macromolecules occurred in the presence of multivalent cations such as Ca^{2+} (Zhang et al., 2009; Chen et al., 2007). Although numerous studies show that relatively subtle changes in water chemistry have been linked to differences in reactivity, bioavailability, and potential toxicity of AgNPs in aquatic environments (Liu et al., 2014; Zhang et al., 2012; Li et al., 2011b), the roles of water chemistry in the mode of antimicrobial action of AgNPs on filamentous fungi have not been addressed systematically in the literature. Therefore, studies on the antifungal efficacy of AgNPs over a wide range of environmental parameters are important to elucidate the effects of AgNPs on microorganisms in ecosystems.

The objective of the current study is to establish a correlation between water characteristics and tolerance of *Phanerochaete chrysosporium* (*P. chrysosporium*, the model species of white-rot fungi) to AgNPs that could easily predict antimicrobial properties and ecotoxicology of AgNPs. Herein, tolerance is defined as cell survival upon antimicrobial treatments. A viability-based tolerance assay was carried out to systematically assess antimicrobial efficacy of AgNPs against *P. chrysosporium* following exposure to different electrolytes including single monovalent, single divalent, a mixture of the two ions, and HA. This study also investigated changes of AgNP size and zeta-potential, dissolved Ag^+ concentration, intracellular and extracellular Ag content, lignolytic enzyme activity, and microbial morphology. Toxicity of Ag^+ versus AgNPs was compared by conducting antibacterial assays under similar water chemistry conditions. Their differential effects on AgNP vs Ag^+ toxicity will be valuable in addressing how water characteristics may affect their relative contributions to AgNP antimicrobial activity.

2. Materials and methods

2.1. Effects of environmental electrolytes on toxicity responses of P. chrysosporium to AgNPs and Ag^+

Influences of monovalent, divalent ions, and HA on AgNP cytotoxicity were investigated in *P. chrysosporium*. To achieve an identical cell concentration, equivalent mycelia (0.2 g) were added respectively into: (i) suspensions containing various concentrations of single electrolytes (0.5–500 mM; NaCl, $NaNO_3$, Na_2SO_4, KCl, KNO_3, K_2SO_4, $CaCl_2$, $Ca(NO_3)_2$, $CaSO_4$, $MgCl_2$, and $MgSO_4$) under 30-μM AgNP stress; (ii) suspensions comprising different AgNP doses (0, 10, 60, 100, and 170 μM) and a constant concentration of the above single electrolytes (30 mM); (iii) mixtures of electrolytes (500 mM $NaNO_3$ and 10 mM $Ca(NO_3)_2$; 500 mM $NaNO_3$ and 100 mM $Ca(NO_3)_2$) with 30 μM AgNPs, higher concentrations of monovalent cations selected were due to their more abundance in the environment and less efficiency in inducing nanoparticle aggregation; and (iv) suspensions consisting of 30 mM of the above single electrolytes, 30 μM AgNPs, and 0.1 g/L HA. Ag^+-elicited toxicity responses were performed similarly under the same conditions except for the substitution of Ag^+ (3 μM) added as $AgNO_3$ for AgNPs (30 μM). The samples were incubated for 24 h at 37 °C. The fungal mycelia were harvested by centrifugation and washed three times with ultrapure water for AgNP/Ag^+ cytotoxicity assessment. Dose-response effects of AgNP/Ag^+ antimicrobial viability were carried out in 2 mM $NaHCO_3$ buffer solution, which was selected due to the fact that it had no influence on silver bioavailability and avoided ligands that might bind with AgNPs and Ag^+ and facilitate precipitation or other confounding effects (Xiu et al., 2012, 2011).

P. chrysosporium strain was cultivated in Kirk's liquid culture medium (Kirk et al., 1978). AgNPs (coated with citrate), with a mean hydrodynamic diameter of 21.6 ± 0.3 nm and a negative zeta-potential of –34.5 ± 1.5 mV, were synthesized by $NaBH_4$ reduction of $AgNO_3$, following the modified procedure as described in our previous studies (Huang et al., 2017, 2018a). Viability of *P. chrysosporium* cells was determined by using the MTT reduction assay according to Chen et al. (2014). Lignin peroxidase (LiP) and manganese peroxidase (MnP) activities were also determined according to our previous report (Huang et al., 2018a). Detailed descriptions on cultivation of *P. chrysosporium*, synthesis and characterization of AgNPs, determination of cellular viability and total Ag content are available in Supporting information.

2.2. Statistical analyses

Statistical analyses were determined by one-way analysis of variance (ANOVA) using Student's t test and differences between treatments were regarded to be significant at $p < 0.05$. All the experiments were repeated independently in triplicate. The results obtained were

presented as the mean of three independent replicates and all data were analyzed with SigmaPlot 14.0 software and SPSS software.

3. Results and discussion

3.1. Effects of different electrolytes on microbial tolerance to AgNPs

Environmental anions may significantly influence the physicochemical properties of AgNPs, and thereby their toxicity (Guo et al., 2017). Survival of *P. chrysosporium* was determined in the presence of AgNPs over a series of monovalent and divalent electrolyte concentrations (Fig. 1). After addition of Na^+, *P. chrysosporium* survival in the presence of 1 mM NaCl increased by 15.4% and 11.7% compared with the control and the treatment with AgNPs alone (103.7%, shown in Section 3.5, Fig. 6A), respectively, whereas a decline in cell viability was observed with an increase in NaCl concentrations from 1 to 100 mM (Fig. 1A). A further increase of Na^+ concentration to 500 mM led to a viability increase for NaCl, Na_2SO_4, and $NaNO_3$. At the same electrolyte concentrations, although *P. chrysosporium* viability in the presence of NaCl was slightly higher than those in Na_2SO_4 and $NaNO_3$, insignificant influence was observed for the three Na^+ dominant suspensions. In the presence of K^+, viability of *P. chrysosporium* in the range of 59.0%–84.6% was almost unchanged for KCl, KNO_3, and K_2SO_4, independent of K^+ concentrations, except for the case of 500 mM KNO_3 with the minimum cell viability of 28.8% (Fig. 1B). The contrasting responses in cell survival between NaCl and KCl amendments indicated the relative preferential interaction/binding of Na^+ as low as 1 mM with carboxylates (COO–) on AgNP surfaces, leading to relative lower bioavailability and cytotoxicity of AgNPs towards *P. chrysosporium* (Pokhrel et al., 2014b). K^+ induced preferential enhancement in AgNP toxicity over Na^+, possibly resulting from a large amount of Ag^+ released from AgNPs upon addition of K^+ (Table 1). Furthermore, the mean hydrodynamic diameters of AgNPs were 37.7 ± 1.6, 41.9 ± 0.6, and 36.0 ± 0.9 nm in the presence of buffer and 1 mM NaCl/KCl electrolytes, respectively. Substantial toxicological studies have documented that AgNPs with relatively larger sizes are much less reactive and toxic than smaller ones, further causing lower adsorption, uptake, and cytotoxicity (Zhao and Wang, 2012; Gliga et al., 2014; Osborne et al., 2015; Chen et al., 2015b). Hence, another possibility for an enhancement in cell viability in 1 mM NaCl electrolyte was the aggregation of nanoparticles.

Survival of *P. chrysosporium* in Ca^{2+} and Mg^{2+} solutions is presented in Fig. 1C and D. Similar to the toxicity profile obtained in the presence of Na^+, cell viability in divalent electrolytes was stimulated by Cl^- at low concentrations (1 mM), but was depressed by almost all of the investigated NO_3^- and SO_4^{2-} concentrations (0.5–30 mM). However, higher concentrations of $CaCl_2$ and $MgCl_2$ electrolytes (30 mM) resulted in cell death with approximately 26.7% and 22.4% of the total cells, respectively, causing certain toxic effects on *P. chrysosporium*. Besides, higher levels of dissolved Ag^+ concentrations were also observed in the presence of 30 mM Cl^- electrolytes (Table 1). Thus, our data indicated that high Cl^- concentrations might drive AgNP dissolution, further exerting the increased toxicity to cells (Chambers et al., 2014).

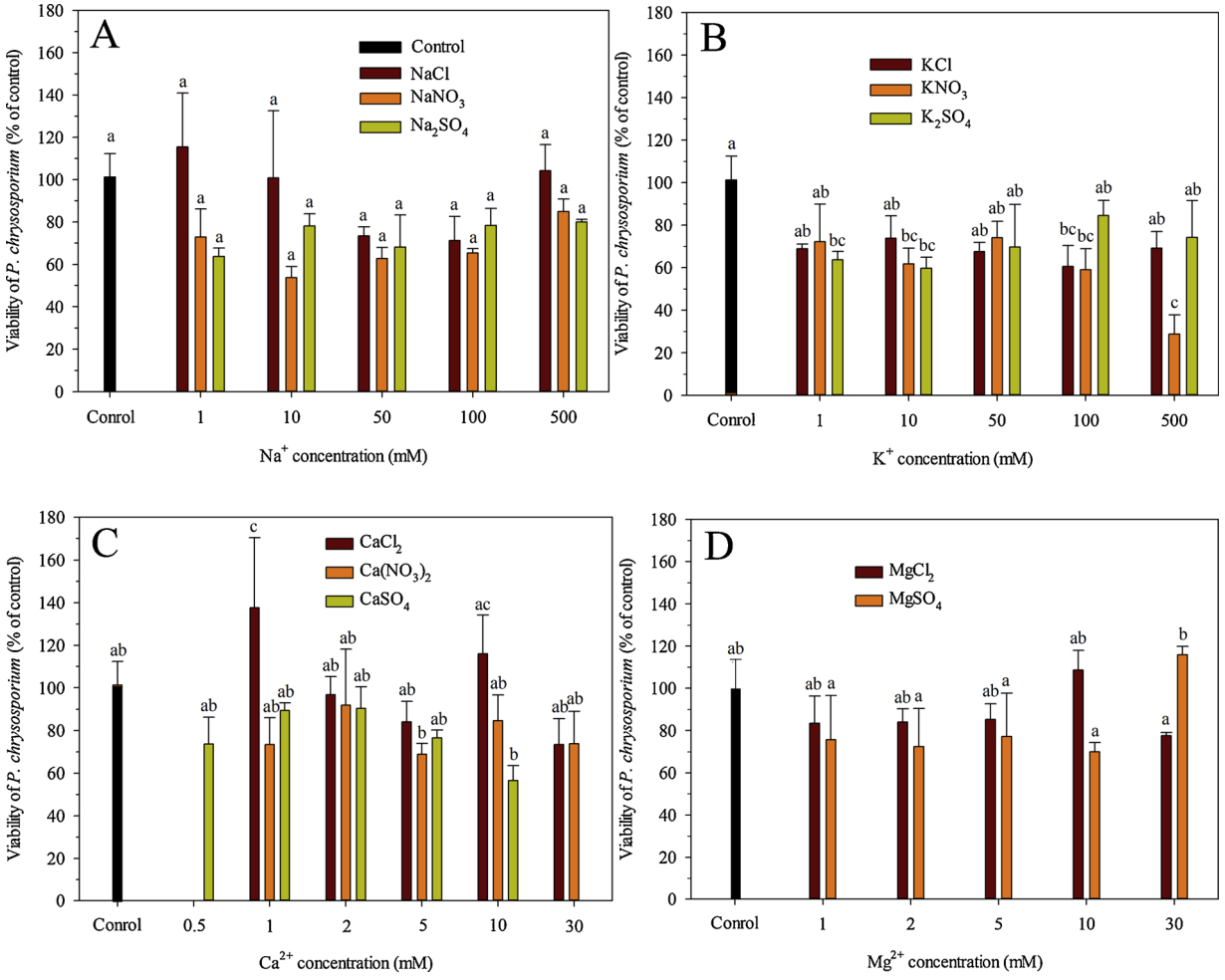

Fig. 1. Effects of (A) Na^+ electrolytes, (B) K^+ electrolytes, (C) Ca^{2+} electrolytes, and (D) Mg^{2+} electrolytes on viability of *P. chrysosporium* under 30-μM AgNP stress. Different letters mean significance of difference between the treatments ($p < 0.05$).

Table 1
Ag^+ concentrations released from 30 μM AgNPs with different electrolytes at concentrations of 1 – 30 mM after 24 h of exposure.

Electrolyte concentration (mM)	Dissolved Ag^+ concentrations (μM)						
	Control[a]	KNO_3	K_2SO_4	KCl	NaCl	$CaCl_2$	$MgCl_2$
0	0.29 ± 0.02						
1		1.54 ± 0.42	1.62 ± 0.56	1.51 ± 0.32	0.25 ± 0.08	0.24 ± 0.03	1.62 ± 0.38
10		1.43 ± 0.24	1.65 ± 0.63	1.56 ± 0.64	0.27 ± 0.04	0.28 ± 0.02	0.25 ± 0.04
30		1.50 ± 0.35	1.44 ± 0.58	1.45 ± 0.91	1.39 ± 0.52	1.53 ± 0.47	1.57 ± 0.46

Control[a] is Ag^+ concentration released from 30 μM AgNPs in the 2 mM $NaHCO_3$ buffer solution.

3.2. Dose-response effects of AgNP antimicrobial viability

Toxicity of AgNPs at various doses towards *P. chrysosporium* in various electrolyte solutions was also evaluated (Fig. 2). In the absence of AgNPs/Ag^+, activity of fungal cells was inhibited by monovalent electrolytes, but promoted considerably by divalent electrolytes. As shown in Fig. 2A, remarkable stimulation in *P. chrysosporium* survival is evoked by 1 and 10 μM AgNPs in the presence of 2 mM $NaHCO_3$ buffer solution, with the increase of 53.2% and 25.7% in microbial viability with respect to the control, respectively. On the contrary, adding $NaNO_3$ increased *P. chrysosporium* survival by 8.0% and 57.8% at AgNP concentrations of 100 and 170 μM, respectively, which were toxic to *P. chrysosporium* in the absence of $NaNO_3$. By comparison, KNO_3 affected insignificantly AgNP toxicity profiles. Obviously, addition of monovalent electrolytes disrupted the stimulatory effects of low-dose AgNPs, while tolerance of *P. chrysosporium* to high-dose AgNPs was greatly improved by the presence of Na^+. These findings also suggested the preference of Na^+ over K^+ to inhibition on the toxic properties of AgNPs, in line with the results obtained in Fig. 1A.

Fig. 2B shows the toxic effects of AgNPs at various concentrations on *P. chrysosporium* survival in the presence of divalent electrolytes. Survival of *P. chrysosporium* increased by 84.1%–123.0% and 18.8%–87.7% for $CaCl_2$ and $Ca(NO_3)_2$, and 23.8%–63.3% and 30%–35.2% for $MgCl_2$ and $MgSO_4$, respectively. However, $MgSO_4$ addition caused a decrease in cell viability (23.9%–36.5%) relative to the control under AgNP doses of 60–170 μM. We found that the increases in *P. chrysosporium* viability were basically greater in Cl^- solutions than in NO_3^- and SO_4^{2-} solutions in the presence of Ca^{2+}/Mg^{2+} and AgNPs, as indicated in Figs. 1 and 2. The lower viability of *P. chrysosporium* was observed in SO_4^{2-} electrolytes, likely due to greater efficiency of SO_4^{2-} in countering the destabilizing effects of Ca^{2+} and Mg^{2+} compared to Cl^- (Liu et al., 2013). More importantly, a noticeable higher increase in cell survival was observed in Ca^{2+} electrolytes compared with Mg^{2+} electrolytes, indicating that Ca^{2+} induced more effective cell protection than the same amount of Mg^{2+} did. This could be explained by the fact that by comparison with Mg^{2+}, Ca^{2+} appeared to act as a constituent of the structural components of microbes more frequently (Sahalan et al., 2013), and that the propensity of Ca^{2+} to form complexes with citrate molecules on the surfaces of AgNPs was higher than that of Mg^{2+}, as evident from a higher stability constant of monodentate Ca^{2+}-citrate complexes relative to monodentate Mg^{2+}-citrate complexes at 25 °C and ionic strength of 0 mM ($10^{1.4}$ versus $10^{1.0}$) (Baalousha et al., 2013; Huynh and Chen, 2011). Furthermore, higher AgNP sizes and lower dissolved Ag^+ concentrations were observed in $CaCl_2$ electrolyte relative to $MgCl_2$ electrolyte (Fig. 3B and Table 1). These findings can also indicate stronger interaction of Ca^{2+} with citrate coating than Mg^{2+} indirectly.

Combined with the observations in Fig. 2A and B, cell survival in Ca^{2+} and Mg^{2+} electrolytes was much higher than that obtained in Na^+ and K^+ electrolytes, especially at low concentrations of AgNPs, indicating that AgNP toxicity to *P. chrysosporium* was reduced by Ca^{2+} and Mg^{2+} more effectively. The reduction of AgNP cytotoxicity could be attributed to the fact that the presence of Ca^{2+} and Mg^{2+} partially neutralized the surface charges of both negatively charged AgNPs and *P. chrysosporium* cells through specific interactions with COO– of the adsorbed citrate molecules on AgNP surfaces and biomacromolecules on the cell surfaces (Table S1). Ca^{2+}/Mg^{2+} neutralization caused the occurrence of partial aggregation of nanoparticles as well, leading to attenuation in direct contact between AgNPs and fungal cells (Xiu et al., 2011).

3.3. Effects of different electrolytes on AgNP stability

When monovalent or divalent electrolytes (30 mM) were added into various concentrations of AgNP suspensions for 24 h, the average hydrodynamic size of AgNPs was determined to estimate nanoparticle stability (Fig. 3). Upon exposure to higher concentrations of AgNPs (100–170 μM), $NaNO_3$ caused a 1.8–2.3-fold increase in nanoparticle average size relative to their corresponding average sizes in buffer solutions, whereas a negligible increase was measured in AgNP size under stress of 60 μM AgNPs (Fig. 3A). KNO_3 did not affect the average sizes of AgNPs, except for a decrease in the average size under 10-μM AgNP

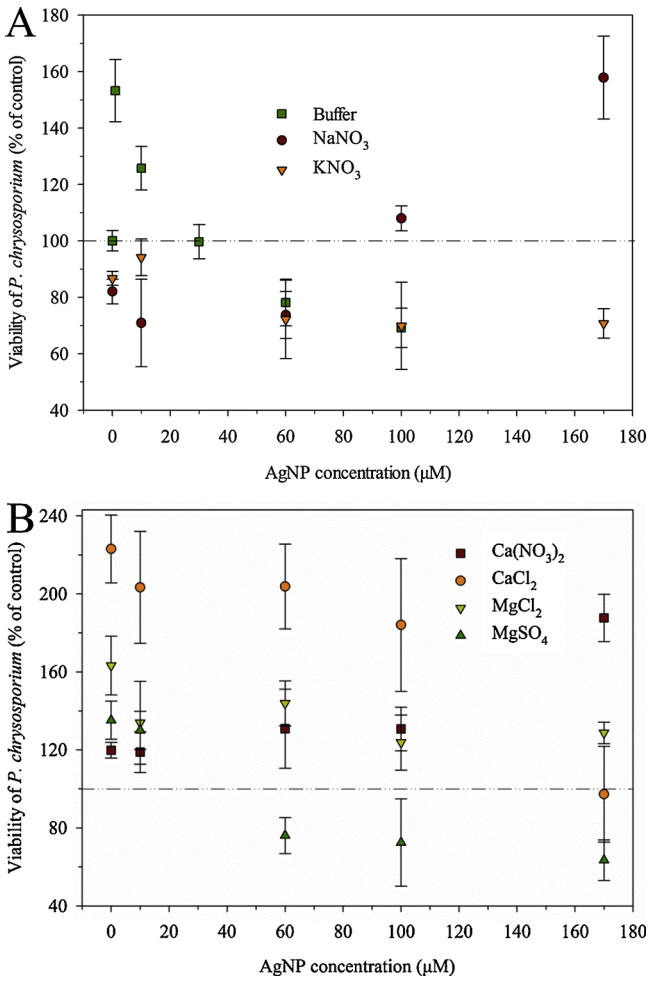

Fig. 2. AgNP toxicity to *P. chrysosporium* in 30 mM (A) monovalent and (B) divalent electrolyte solutions. The buffer was 2 mM $NaHCO_3$ buffer solution.

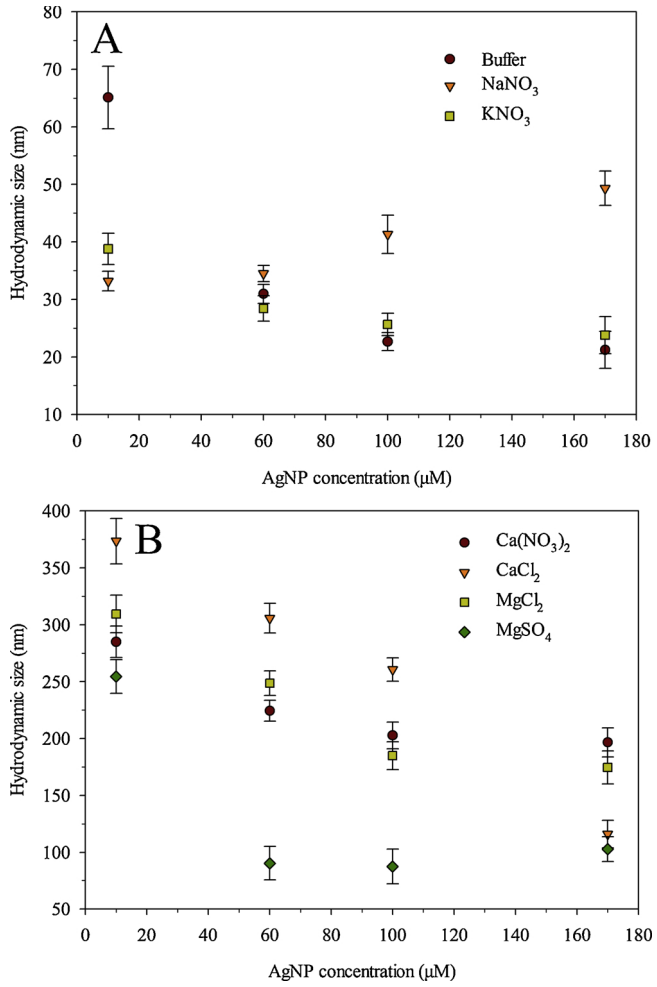

Fig. 3. Hydrodynamic size (nm) of AgNPs in (A) monovalent and (B) divalent electrolytes at concentrations of 30 mM after 24 h of contact.

stess. Presumably, monovalent electrolytes maintained and enhanced the nanoparticle stability, especially in K^+ electrolytes. However, Ca^{2+}/Mg^{2+} electrolytes induced a significant increase of 2.9–11.5 folds in the average size of AgNPs compared to their corresponding sizes in the buffer (Fig. 3B). In comparison with Ca^{2+} electrolytes, lower AgNP sizes were evoked by $MgSO_4$. The rise in AgNP average size in the presence of divalent electrolytes suggested potential aggregation/agglomeration of AgNPs (Huang et al., 2018b), which was consistent with the changes in *P. chrysosporium* viability in Figs. 1 and 2.

3.4. Effects of different electrolytes on microbial tolerance to Ag^+

Numerous studies have shown that antimicrobial properties of AgNPs primarily stem from dissolved Ag^+, which can effectively inactivate a wide variety of microbes. To discern the specific contribution of monovalent and divalent electrolytes to AgNP toxicity, the antimicrobial assays of Ag^+ ions were carried out under the conditions of the same electrolyte solutions (Fig. 4). As noted in Fig. 4A, survival of *P. chrysosporium* exposed to 3 μM Ag^+ was enhanced upon addition of 50 mM NaCl and 10 mM Na_2SO_4, increasing by 10.2% and 9.3% relative to the control, respectively. However, *P. chrysosporium* survivals in 500 mM NaCl and Na_2SO_4 solutions were only 30.0% and 51.7%, respectively. These results indicated that toxicity of Ag^+ cannot be counteracted by adding excess Cl^- and SO_4^{2-}. Another possibility was that salt shock (osmotic stress) led to a decrease in cell activity at the higher Na^+ concentrations. Furthermore, $NaNO_3$ amendment did not markedly affect Ag^+ antimicrobial ability. Similarly, no significant alteration in antimicrobial activity was observed with the addition of K^+, except for treatments with 10 mM KNO_3 and 500 mM KCl/KNO_3/K_2SO_4 (Fig. 4B).

Survival of fungal cells in the presence of Ag^+ and divalent electrolytes is presented in Fig. 4C and D. The results indicated that *P. chrysosporium* viability under the same ionic strengths followed the order: in SO_4^{2-} > Cl^- > NO_3^- electrolyte solutions, without obvious variations over a series of Ca^{2+} and Mg^{2+} concentrations investigated. Additionally, in the absence of electrolytes, a concentration of 3 μM Ag^+ diminished the microbial survival, causing 53.7% of the total cells being killed (seen in Section 3.6, Fig. 6B). By contrast, it was found that SO_4^{2-} and Cl^- exhibited a stimulatory effect on microbial viability with respect to Ag^+ alone and that toxic effects of Ag^+ to cells can be negligibly influenced by NO_3-. It is widely accepted that Ag^+ bioavailability is hindered by forming complexation and/or precipitation with SO_4^{2-} and Cl^- in the media, e.g., relatively insoluble Ag_2SO_4 and AgCl molecules. Additionally, it is well-known that Cl^- has a relatively lower solubility product equilibrium constant than SO_4^{2-} ($K_{sp\text{-}AgCl} = 1.8 \times 10^{-10}$ and $K_{sp\text{-}Ag2SO4} = 1.2 \times 10^{-5}$) (Levard et al., 2012). And in comparison with Ag_2SO_4, the solubility product constant of AgCl was exceeded by our tested concentrations (1.8×10^{-7}), indicating that the formation of AgCl was much more stable than Ag_2SO_4. In that case, more significant toxicity reduction should be observed by Cl^-, rather than SO_4^{2-}, which was obviously opposite to the findings in the present work. Comparison of their stability constants and potential to reduce Ag^+ toxicity suggested that for the higher Cl/Ag molar ratios, it was likely for the formation of soluble $AgCl_{(aq)}$ or $AgCl_2^-$, as well as $AgCl_3^{2-}$ and $AgCl_4^{3-}$ below the precipitation potential, because the toxicity of Ag^+ was not completely removed by the addition of Cl^- (Levard et al., 2012). This speculation can be verified by observation in distribution of total Ag content in Fig. S1. Total extracellular Ag content was considerably suppressed to an undetectable level upon addition of $CaCl_2$/$MgCl_2$ into AgNP and Ag^+ suspensions (Fig. S1A and B). However, an increase in total intracellular Ag content was observed upon $CaCl_2$ amendment of Ag^+; by contrast, total intracellular Ag content under AgNP exposure was not detected (Fig. S1C). Unlike Cl^-, mitigation of SO_4^{2-} on toxic effects of Ag^+ probably originated from the complexation of SO_4^{2-} with Ag^+, and the aqueous and unstable complexes might lead to a fluctuation in microbial survival to a certain extent.

3.5. Dose-response effects of Ag^+ on cell viability

Influences of monovalent and divalent electrolytes on Ag^+ dose-response toxicity against *P. chrysosporium* are presented in Fig. 5. A similar trend as for different amount of AgNPs in the presence of KNO_3 was observed for dose-response curves of Ag^+ in microbial viability with monovalent electrolytes (Fig. 5A). $NaNO_3$ and KNO_3 did not significantly affect the toxic effects of Ag^+ towards cells, except for the inhibition at low Ag^+ concentrations (0–1 μM) that showing a stimulatory effect in the absence of electrolytes, and their corresponding EC_{50} values were statistically undistinguishable ($p > 0.05$) (EC_{50}: 1.4 vs 4.9 μM) relative to buffer exposure (EC_{50}: 4.6 μM). In contrast to $NaNO_3$/KNO_3 electrolytes, the presence of $CaCl_2$ (EC_{50}: 8.2 μM), $MgCl_2$ (EC_{50}: 12.4 μM), and $MgSO_4$ (EC_{50}: 7.8 μM) alleviated the toxic action of Ag^+ at concentrations of 0–3 μM to some extent (Fig. 5B). Nevertheless, *P. chrysosporium* survival upon $Ca(NO_3)_2$ amendment was still depressed, similar to that upon amendments of $NaNO_3$ and KNO_3. These results demonstrated that antimicrobial toxicity of Ag^+ to *P. chrysosporium* was evidently enhanced by NO_3^- under low doses of Ag^+, regardless of monovalent or divalent cations, but was inhibited upon addition of Cl^- and SO_4^{2-} electrolytes. Upon further increases in Ag^+ concentrations, the microbiocidal effects of Ag^+ on *P. chrysosporium* were not easily subjected to the influence of all the monovalent and divalent electrolytes, probably due to the bioavailability and cytotoxicity of the formation of soluble and/or unstable silver species. Moreover, on the basis of EC_{50} values, Ag^+ ions were about 28× more toxic to *P. chrysosporium* than AgNPs in the buffer solutions (Figs. 2A and 5A) (EC_{50}: 4.6 vs 126.9 μM).

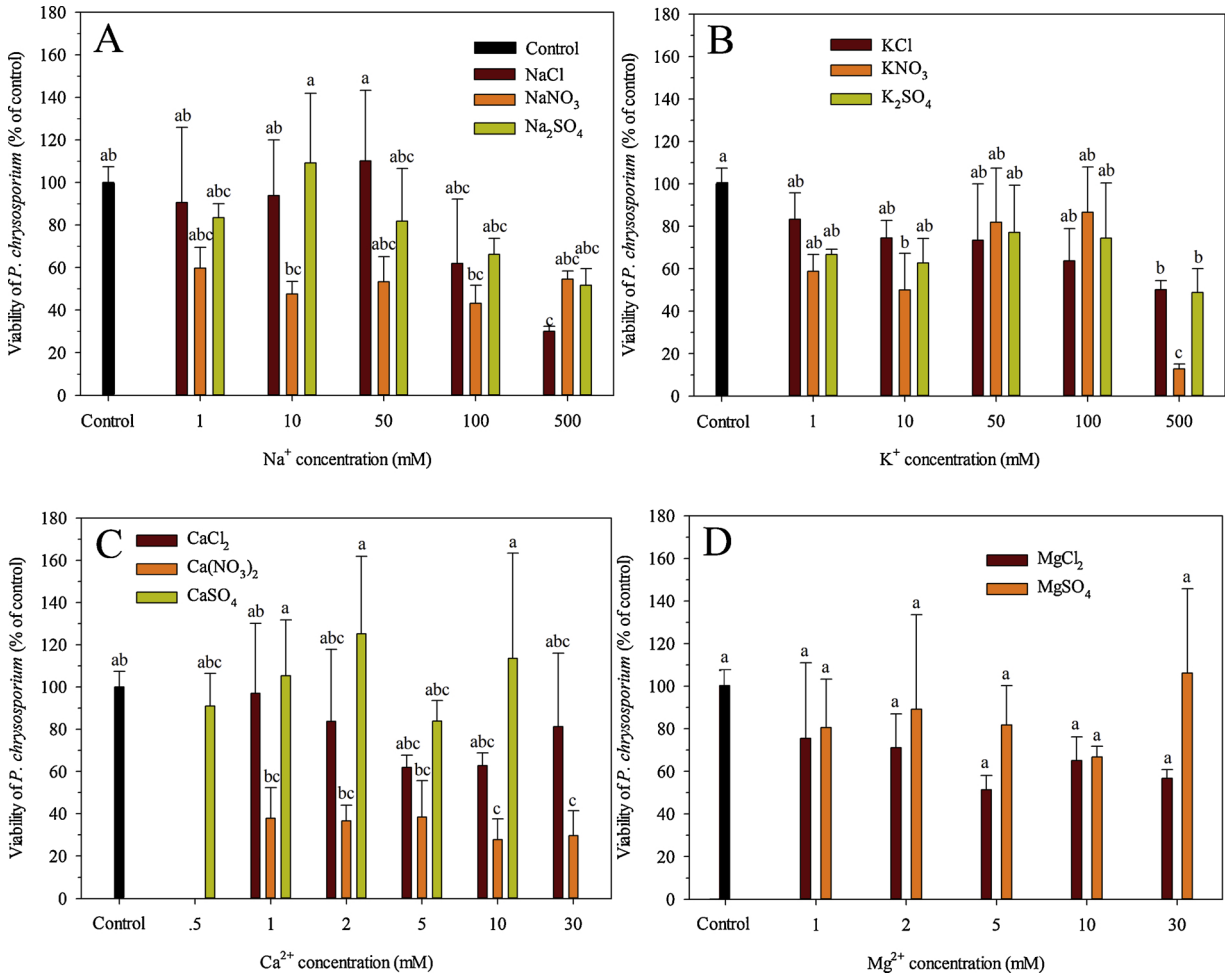

Fig. 4. Effects of (A) Na^+ electrolytes, (B) K^+ electrolytes, (C) Ca^{2+} electrolytes, and (D) Mg^{2+} electrolytes on viability of *P. chrysosporium* under 3-μM Ag^+ stress. Different letters mean significance of difference between the treatments ($p < 0.05$).

Besides, the toxicity of AgNPs and Ag^+ to *P. chrysosporium* presented a time-dependent decrease, and in contrast with divalent electrolytes, monovalent electrolytes elicited a more significant decrease in cell survival (Fig. S2). Meanwhile, under AgNP stress, there was no significant difference in LiP activities between the samples in $NaNO_3$/KNO_3/$MgSO_4$ and buffer solutions; however, LiP activity was significantly stimulated upon addition of $Ca(NO_3)_2$, $CaCl_2$, and $MgCl_2$ (Fig. S3A). A significant stimulation in LiP activity was also induced after addition of $CaCl_2$/$MgCl_2$/$MgSO_4$ into Ag^+ solutions. NO_3^- electrolytes insignificantly influenced LiP activity upon exposure to Ag^+, relative to those in the control and buffer. The alterations of MnP activity under stresses of AgNPs and Ag^+ with various electrolytes were similar to those of LiP (Fig. S3B). Coupled with the analyses of influences of different electrolytes on microbial tolerance to AgNPs/Ag^+ and dose-response effects of AgNP/Ag^+ on cell viability, predictably, it was also observed that higher viabilities under AgNP exposure were induced by divalent electrolytes with the preference of Ca^{2+} over Mg^{2+}, compared to monovalent electrolytes. And viability of *P. chrysosporium* treated with low-dose Ag^+ was indeed inhibited by NO_3^- electrolytes, but was enhanced by Cl^- and SO_4^{2-} electrolytes.

3.6. AgNP/Ag^+ toxicity in the presence of mixture of mono and divalent electrolytes

Tolerance of *P. chrysosporium* to AgNPs and Ag^+ showed an apparent disparity in the presence of single and combined electrolytes of $NaNO_3$ and $Ca(NO_3)_2$ (Fig. 6). As shown in Fig. 6A, the antimicrobial effectiveness of AgNPs can be enhanced by 500 mM $NaNO_3$ alone, 10 mM $Ca(NO_3)_2$ alone, and the combination of the two; however, introduction of 100 mM $Ca(NO_3)_2$ into 500 mM $NaNO_3$ solutions mitigated the toxicity of AgNPs to *P. chrysosporium*. Thus, the dominance of $Ca(NO_3)_2$ at high concentrations in controlling AgNP behaviors (e.g. aggregation) in this mixture can be concluded. In marked contrast to the observations made under AgNP stress, negligible impacts of $NaNO_3$ and $Ca(NO_3)_2$, separately and in combination, on Ag^+ antimicrobial effects were observed in Fig. 6B.

Besides, in order to visualize the influence of $Ca(NO_3)_2$ on AgNP/Ag^+ antimicrobial efficacy in the presence of mixture of mono and divalent electrolytes, membrane damage of *P. chrysosoporium* cells was determined after uniform dyeing with propidium iodide. In the presence of 500 mM $NaNO_3$, weaker red fluorescence under AgNP stress was shown when *P. chrysosporium* was exposed to 100 mM $Ca(NO_3)_2$ in comparison to10 mM $Ca(NO_3)_2$ (Fig. S4A and B). This implied that addition of high-concentration $Ca(NO_3)_2$ triggered less loss of plasma membrane and improved viability of *P. chrysosporium* exposed to AgNPs. However, an opposite phenomenon was observed under stress of Ag^+ (Fig. S4C and D). Meanwhile, it was also found that *P. chrysosporium* cells showed stronger red fluorescence after addition of 100 mM $Ca(NO_3)_2$ into the Ag^+ solution as well as 500 mM $NaNO_3$ than that challenged with 10 mM $Ca(NO_3)_2$. Apparently, addition of high-level $Ca(NO_3)_2$ in the presence of $NaNO_3$ lowered AgNP cytotoxicity, leading to unobvious damage of plasma damage, in agreement with the observations of Fig. 6.

The results from Figs. 6 and S4 manifested that environmental electrolytes modulated the toxicity of AgNPs and Ag^+ via specific chemical interactions differentially, thus affecting their relative contributions to antimicrobial activity. Furthermore, it was found that higher dissolved Ag^+ concentrations were obtained in the electrolytes

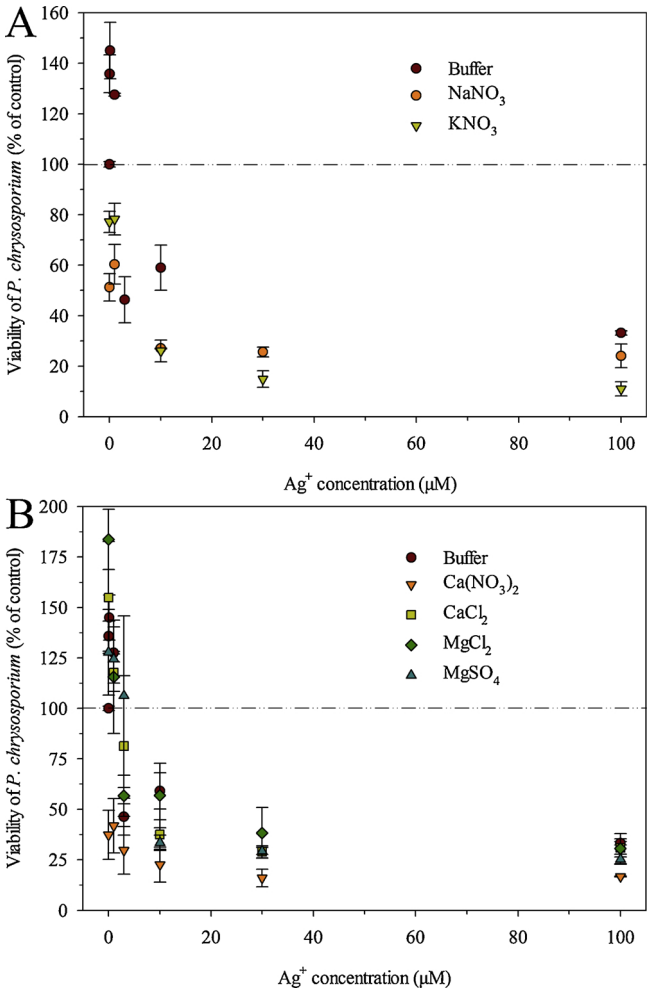

Fig. 5. Ag^+ toxicity to *P. chrysosporium* in 30 mM (A) monovalent and (B) divalent electrolyte solutions. The buffer was 2 mM $NaHCO_3$ buffer solution.

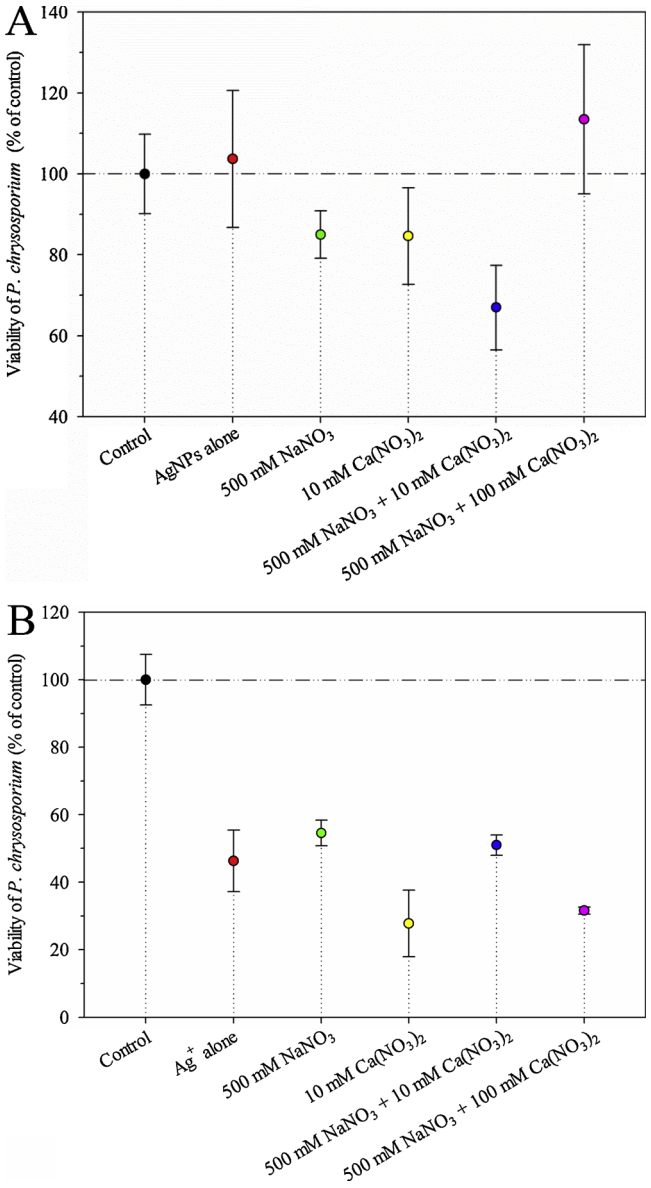

Fig. 6. Viability of *P. chrysosporium* in single $NaNO_3$, single $Ca(NO_3)_2$, and the combination of both under stress of (A) 30 μM AgNPs and (B) 3 μM Ag^+.

of 500 mM $NaNO_3$ and/or 10 mM $Ca(NO_3)_2$, and that there was a larger hydrodanamic size in the mixture of 500 mM $NaNO_3$ and100 mM $Ca(NO_3)_2$ relative to those in the buffer (Table S2). Predictably, lower survival of *P. chrysosporium* possibly arose from a large amount of Ag^+ released from AgNPs in the presence of monovalent cations and/or low concentrations of divalent cations. However, AgNP aggregation might be predominantly induced under higher concentrations of divalent cations, thereby showing higher *P. chrysosporium* survival.

3.7. Effects of electrolytes and HA coexistence on AgNP/Ag^+ toxicity

NOM may exist together with various cations and anions in natural or engineered aquatic and soil systems. Here, the comprehensive effects on antimicrobial efficacy of AgNPs and Ag^+ caused by combination of HA and electrolytes were investigated (Fig. 7). The microbial viabilities of samples in the HA alone and AgNP alone systems were slightly higher than that in the control (Fig. 7A). The decreased viability of *P. chrysosporium* in electrolyte solutions (except $MgSO_4$) without HA was observed under AgNP stress relative to the control. But the mixture of HA and NaCl, Na_2SO_4, $Ca(NO_3)_2$, $CaCl_2$, or $MgCl_2$ electrolytes greatly improved the viability. The observations suggested that HA addition could weaken the enhanced antimicrobial efficacy of AgNPs in these electrolyte solutions. Huang et al. (2016) found that HA might mitigate the anti-algae efficacy of AgNPs to *Microcystis aeruginosa* through changing physicochemical properties and dissolution behavior of nanoparticles. Mitigation of AgNP toxicity by HA was possibly because the adsorption of HA onto the surfaces of AgNPs and *P. chrysosporium* hindered their direct interaction and/or uptake of AgNPs by fungal cells (Tang et al., 2014; Wan et al., 2017; Ren et al., 2018). Considering negatively charged functional groups present on HA macromolecules, HA coating on AgNPs and cells also increased the electrostatic and steric repulsive forces between them due to the more negative surface charges. Meanwhile, the adsorbed HA could inhibit Ag^+ release on account of blockage of active sites, oxidant competition, reduction reactions, or complexation (Huang et al., 2016). In addition, Ca^{2+} and Mg^{2+} have also been found to promote HA adsorption onto AgNP surface (Liu et al., 2013). Complexation of Ca^{2+}/Mg^{2+} with COO– on HA and AgNP surfaces could probably neutralize their negative charged, leading to weaker repulsion between AgNPs and fungal cells and making AgNP

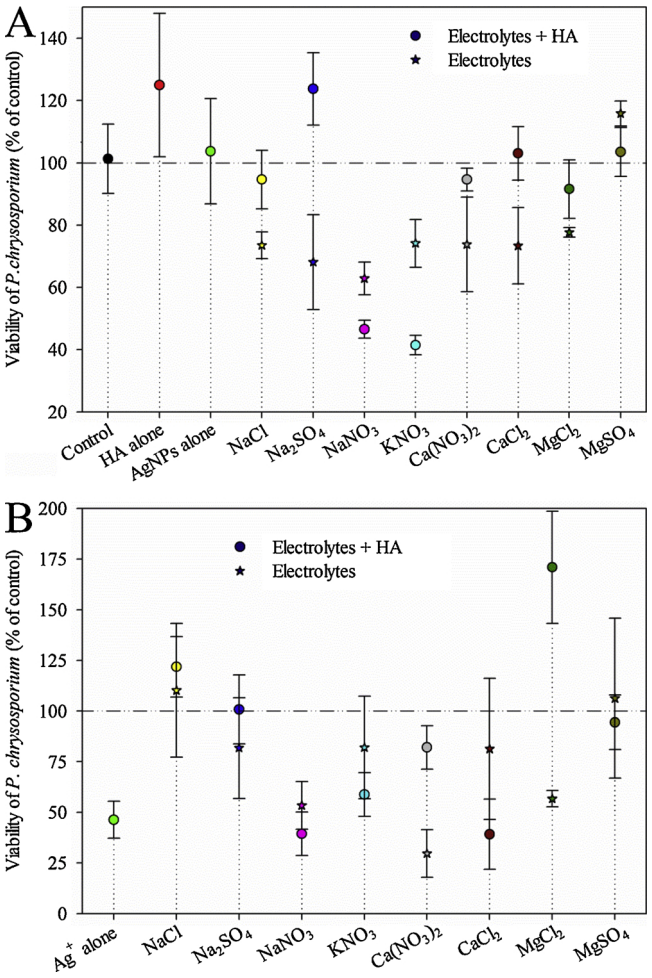

Fig. 7. Viability of *P. chrysosporium* in various electrolyte solutions with and without 0.1 g/L HA under (A) 30-μM AgNP and (B) 3-μM Ag^+ stress.

contact with and bind to fungal cells easier. However, the coating of HA might play a greater role in decreasing the probabilities of direct contact and interaction between nanoparticles and cells, thus alleviating the antimicrobial toxicity of AgNPs (Huang et al., 2016; Liu et al., 2013). Remarkably, the enhancement of AgNP toxicity to *P. chrysosporium* was observed in $NaNO_3$ and KNO_3 electrolytes without HA; however, the coexistence of HA and $NaNO_3$/KNO_3 aggravated the toxicity of AgNPs more significantly, which could be interpreted by the formation of relatively smaller and more stable particles after addition of HA (Fabrega et al., 2009; Schaumann et al., 2015). The results also indicated that the antimicrobial toxicity of AgNPs towards *P. chrysosporium* in the presence of a mixture of HA and $NaNO_3$/KNO_3 might be additive.

For better understanding of the effects of Ca^{2+}/Mg^{2+} and HA addition on AgNPs/Ag^+ stimulation for microbial growth, SEM measurements on the surfaces of control, fungi after treatment with AgNPs alone and combined treatment with AgNPs, Ca^{2+}/Mg^{2+} and HA were conducted (Fig. 8). All the SEM images exhibited network surface structures with smooth mycelia and void spaces between the hyphae. Analysis of AgNP treatment exhibited widened hyphae loaded with some crystal particles compared to the control (Fig. 8A and B). After addition of Ca^{2+}/Mg^{2+} and HA, more vigorous and compact mycelia attached with fewer crystals were observed in the presence of AgNPs in Fig. 8C and D. It reflected that Ca^{2+}/Mg^{2+} and HA addition contributed to stimulation of AgNPs for microbial growth possibly because of the reduction in direct contact, interaction, and uptake of AgNPs/Ag^+ with cell components.

Besides, in Ag^+ solutions, the survival of *P. chrysosporium* in Ca$(NO_3)_2$ and $MgCl_2$ solutions with HA was increased by 52.3% and 114.3% over those without HA, respectively (Fig. 7B). The difference in *P. chrysosporium* survival in Ca$(NO_3)_2$ and $MgCl_2$ was presumably due to complexation of Cl^- with Ag^+. However, apart from the two electrolytes, there was no dramatic change in *P. chrysosporium* viability under Ag^+ stress in all the electrolytes with and without HA addition. Furthermore, adding HA prominently improved the survival of *P. chrysosporium* in $MgCl_2$ solution, but resulted in a slight inhibitory effect on microbial activity in $CaCl_2$ solution. Therefore, the effects of Cl^- present in solutions on Ag^+ toxicity may not be the dominant factor. Meanwhile, the comparison of cell survival in $CaCl_2$ and $MgCl_2$ solutions showed that Mg^{2+} possibly induced a stronger complexation with HA than Ca^{2+} in Ag^+ solution, which was contrary to the previous findings of a lower affinity of Mg^{2+} to COO– of NOM compared to Ca^{2+} (Liu et al., 2013; Pandey et al., 2000). Further studies must be conducted to further explore direct evidence involved. By contrast, for AgNPs, no evidence of a stronger affinity of Mg^{2+} for HA was observed. It was implied that the impacts of divalent electrolytes and NOM might be strongly dependent on the metal species present and that AgNPs could bind to NOM more strongly than Ag^+.

In a word, the toxicity of AgNPs and Ag^+ has been affected differentially by common electrolytes and HA in aquatic systems, further altering their relative contribution to antimicrobial capacities. Previous studies have reported that the interactions of nanoparticles with plasma membranes may lead to particle aggregation, dissolution, and restructuring at the nanomaterial surfaces and play a key role in the antimicrobial effects (Malekkhaiat and Malmsten, 2017; Huang et al., 2018c; Xu et al., 2012a,b). In this study, combined with SEM observations in Fig. 8, the enhanced AgNP stimulation for microbial growth upon addition of Ca^{2+}/Mg^{2+} and in the presence of HA could be attributed to reduction in direct contact, interaction, and uptake of AgNPs/Ag^+ with cell components due to the formation of new surface coatings and particle aggregation. However, antimicrobial performance of AgNPs was enhanced in the presence of monovalent electrolytes, particularly K^+, which might be associated with AgNP dissolution. The action would further aggravate a large amount of Ag^+ release and direct contact/interaction between AgNPs and *P. chrysosporium* cells.

4. Conclusions

In the present study, monovalent electrolytes, especially K^+, enhanced the antimicrobial efficacy of AgNPs, while an obvious promotion in AgNP stimulation of microbial activity was observed in divalent electrolytes. Ca^{2+} induced more effective tolerance of *P. chrysosporium* to AgNPs than the same concentrations of Mg^{2+} did. For combination of monovalent and divalent electrolytes, the dominating factor for AgNP antimicrobial capability was divalent cations. Collectively, it was hypothesized that the major factors responsible for AgNP cytotoxicity towards *P. chrysosporium* were direct contact/interaction and specific reactions between nanoparticles and cells. The enhanced AgNP toxicity in monovalent electrolytes mainly arose from the aggravated nanoparticle-microbe interplay, resulting in Ag^+ dissociation. However, the reduced direct contact and interaction of AgNPs/Ag^+ with cell components due to aggregation, complexation, and HA surface coating greatly mitigated the antimicrobial activity of AgNPs in the presence of divalent electrolytes and HA. The observations here have great implications for better understanding in ecotoxicity of nanomaterials in natural water systems.

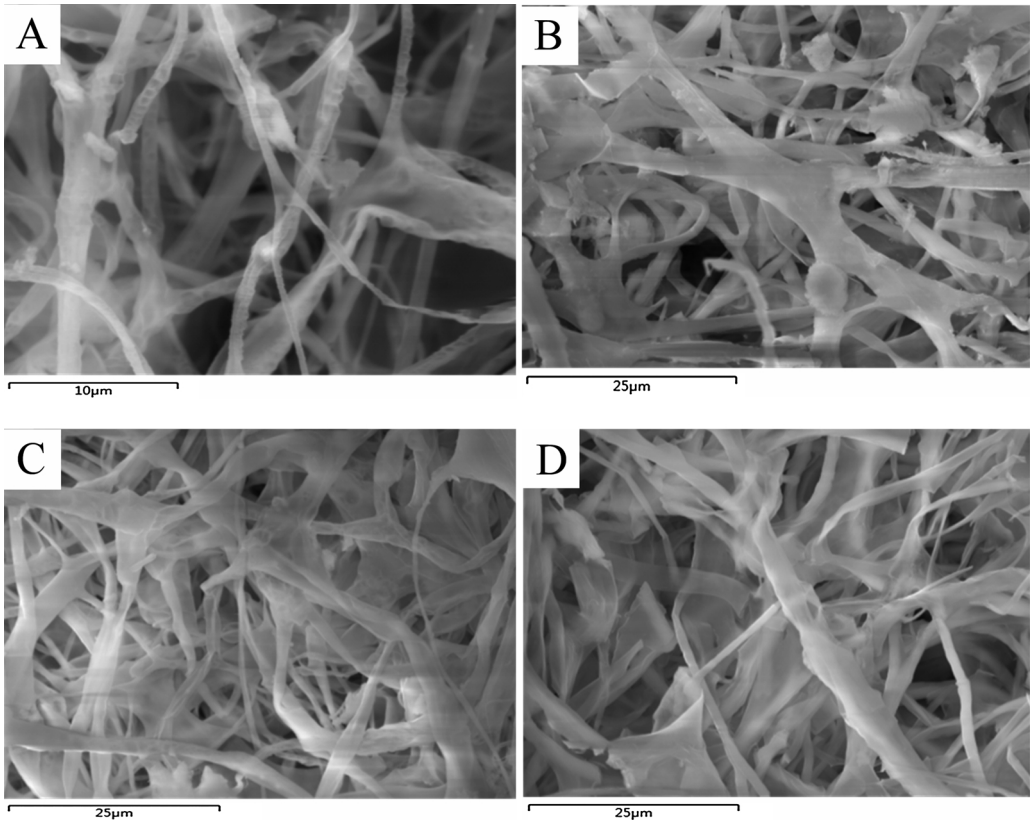

Fig. 8. SEM micrographs of fungal surfaces: (A) control, (B) with single 30 μM AgNPs, (C) 30 mM $CaCl_2$ + 0.1 g/L HA + 30 μM AgNPs, and (D) 30 mM $MgCl_2$ + 0.1 g/L HA + 30 μM AgNPs.

Acknowledgements

This work was financially supported by the National Natural Science Foundation of China (81773333, < GN1 > 51579099, < GN1 > 51521006, and < GN1 > 51508186), the P < /GN1 > < /GN1 > < / GN1 > rogram for Changjiang Scholars and Innovative Research Team in University (IRT-13R17), the Hunan Provincial Natural Science Foundation of China (2016JJ3076), and the Opening Project of Henan Provincial Key Laboratory of Water Pollution Control and Rehabilitation Technology (CJSP2018010).

Appendix A. Supplementary data

Supplementary material related to this article can be found, in the online version, at doi:https://doi.org/10.1016/j.jhazmat.2019.121153.

References

Chambers, B.A., Afrooz, A.R., Bae, S., Aich, N., Katz, L., Saleh, N.B., Kirisits, M.J., 2014. Effects of chloride and ionic strength on physical morphology, dissolution, and bacterial toxicity of silver nanoparticles. Environ. Sci. Technol. 48, 761–769.

Levard, C., Hotze, E.M., Lowry, G.V., Brown, G.E., 2012. Environmental transformations of silver nanoparticles: impact on stability and toxicity. Environ. Sci. Technol. 46, 6900–6914.

He, K., Chen, G., Zeng, G., Huang, Z., Guo, Z., Huang, T., Min, M., Shi, J., Hu, L., 2017. Applications of white rot fungi in bioremediation with nanoparticles and biosynthesis of metallic nanoparticles. Appl. Microbiol. Biotechnol. 101, 4853–4862.

Gong, J.L., Wang, B., Zeng, G.M., Yang, C.P., Niu, C.G., Niu, Q.Y., Zhou, W.J., Liang, Y., 2009. Removal of cationic dyes from aqueous solution using magnetic multi-wall carbon nanotube nanocomposite as adsorbent. J. Hazard. Mater. 164, 1517–1522.

Huang, T., Sui, M., Yan, X., Zhang, X., Yuan, Z., 2016. Anti-algae efficacy of silver nanoparticles to *Microcystis aeruginosa*: influence of NOM, divalent cations, and pH. Colloids Surf. A 509, 492–503.

Li, X., Lenhart, J.J., 2012. Aggregation and dissolution of silver nanoparticles in natural surface water. Environ. Sci. Technol. 46, 5378–5386.

Zhang, Y., Zeng, G.M., Tang, L., Chen, J., Zhu, Y., He, X.X., He, Y., 2015. Electrochemical sensor based on electrodeposited graphene-Au modified electrode and nano Au carrier amplified signal strategy for attomolar mercury detection. Anal. Chem. 87, 989–996.

Liu, J., Hurt, R.H., 2010. Ion release kinetics and particle persistence in aqueous nano-silver colloids. Environ. Sci. Technol. 44, 2169–2175.

Guo, Z., Chen, G., Zeng, G., Ming, Y., Huang, Z., Jiang, L., Peng, C., Wang, J., Xiao, Z., 2017. Are silver nanoparticles always toxic in the presence of environmental anions? Chemosphere 171, 318–323.

Xiu, Z.M., Zhang, Q.B., Puppala, H.L., Colvin, V.L., Alvarez, P.J.J., 2012. Negligible particle-specific antibacterial activity of silver nanoparticles. Nano Lett. 12, 4271–4275.

Zuo, Y., Chen, G., Zeng, G., Li, Z., Yan, M., Chen, A., Guo, Z., Huang, Z., Tan, Q., 2015. Transport, fate, and stimulating impact of silver nanoparticles on the removal of Cd (II) by *Phanerochaete chrysosporium* in aqueous solutions. J. Hazard. Mater. 285, 236–244.

Tan, X., Liu, Y., Zeng, G., Wang, X., Hu, X., Gu, Y., Yang, Z., 2015. Application of biochar for the removal of pollutants from aqueous solutions. Chemosphere 125, 70–85.

Deng, J.H., Zhang, X.R., Zeng, G.M., Gong, J.L., Niu, Q.Y., Liang, J., 2013. Simultaneous removal of Cd(II) and ionic dyes from aqueous solution using magnetic graphene oxide nanocomposite as an adsorbent. Chem. Eng. J. 226, 189–200.

Chen, M., Xu, P., Zeng, G., Yang, C., Huang, D., Zhang, J., 2015a. Bioremediation of soils contaminated with polycyclic aromatic hydrocarbons, petroleum, pesticides, chlorophenols and heavy metals by composting: applications, microbes and future research needs. Biotechnol. Adv. 33, 745–755.

Zhang, C., Wang, W., Duan, A., Zeng, G., Huang, D., Lai, C., Tan, X., Cheng, M., Wang, R., Zhou, C., Xiong, W., Yang, Y., 2019. Adsorption behavior of engineered carbons and carbon nanomaterials for metal endocrine disruptors: experiments and theoretical calculation. Chemosphere 222, 184–194.

Zhou, C., Lai, C., Huang, D., Zeng, G., Zhang, C., Cheng, M., Hu, L., Wan, J., Xiong, W., Wen, M., Wen, X., Qin, L., 2018. Highly porous carbon nitride by supramolecular preassembly of monomers for photocatalytic removal of sulfamethazine under visible light driven. Appl. Catal. B 220, 202–210.

He, D., Zhang, C., Zeng, G., Yang, Y., Huang, D., Wang, L., Wang, H., 2019. A multifunctional platform by controlling of carbon nitride in the core-shell structure from design to construction, and catalysis applications. Appl. Catal. B 258, 117957.

Zhou, H., Wu, S., Zhou, Y., Yang, Y., Zhang, J., Luo, L., Duan, X., Wang, S., Wang, L., Tsang, D.C.W., 2019. Insights into the oxidation of organic contaminants by iron nanoparticles encapsulated within boron and nitrogen co-doped carbon nanoshell: catalyzed Fenton-like reaction at natural pH. Environ. Int. 128, 77–88.

Li, M., Zhu, L.Z., Lin, D.H., 2011a. Toxicity of ZnO nanoparticles to *Escherichia coli*: mechanism and the influence of medium components. Environ. Sci. Technol. 45, 1977–1983.

Jin, X., Li, M.H., Wang, J.W., Marambio-Jones, C., Peng, F.B., Huang, X.F., Damoiseaux, R., Hoek, E.M.V., 2010. High-throughput screening of silver nanoparticle stability

and bacterial inactivation in aquatic media: influence of specific ions. Environ. Sci. Technol. 44, 7321–7328.
Long, F., Gong, J.L., Zeng, G.M., Chen, L., Wang, X.Y., Deng, J.H., Niu, Q.Y., Zhang, H.Y., Zhang, X.R., 2011. Removal of phosphate from aqueous solution by magnetic Fe–Zr binary oxide. Chem. Eng. J. 171, 448–455.
Tejamaya, M., Römer, I., Merrifield, R.C., Lead, J.R., 2012. Stability of citrate, PVP, and PEG coated silver nanoparticles in ecotoxicology media. Environ. Sci. Technol. 46, 7011–7017.
Deonarine, A., Lau, B.L.T., Aiken, G.R., Ryan, J.N., Hsu-Kim, H., 2011. Effects of humic substances on precipitation and aggregation of zinc sulfide nanoparticles. Environ. Sci. Technol. 45, 3217–3223.
Anderson, J.W., Semprini, L., Radniecki, T.S., 2014. Influence of water hardness on silver ion and silver nanoparticle fate and toxicity toward *Nitrosomonas europaea*. Environ. Eng. Sci. 31, 403–409.
Zhang, H.Y., Oyanedel-Craver, V., 2012. Evaluation of the disinfectant performance of silver nanoparticles in different water chemistry conditions. J. Environ. Eng. 138, 58–66.
Pokhrel, L.R., Dubey, B., Scheuerman, P.R., 2014a. Natural water chemistry (dissolved organic carbon, pH, and hardness) modulates colloidal stability, dissolution, and antimicrobial activity of citrate functionalized silver nanoparticles. Environ. Sci. Nano 1, 45–54.
Xiu, Z.M., Ma, J., Alvarez, P.J.J., 2011. Differential effect of common ligands and molecular oxygen on antimicrobial activity of silver nanoparticles versus silver ions. Environ. Sci. Technol. 45, 9003–9008.
Li, X., Lenhart, J.J., Walker, H.W., 2010. Dissolution-accompanied aggregation kinetics of silver nanoparticles. Langmuir 26, 16690–16698.
Liang, J., Yang, Z., Tang, L., Zeng, G., Yu, M., Li, X., Wu, H., Qian, Y., Li, X., Luo, Y., 2017. Changes in heavy metal mobility and availability from contaminated wetland soil remediated with combined biochar-compost. Chemosphere 181, 281–288.
Afshinnia, K., Baalousha, M., 2017. Effect of phosphate buffer on aggregation kinetics of citrate-coated silver nanoparticles induced by monovalent and divalent electrolytes. Sci. Total Environ. 581–582, 268–276.
Baalousha, M., Nur, Y., Römer, I., Tejamaya, M., Lead, J.R., 2013. Effect of monovalent and divalent cations, anions and fulvic acid on aggregation of citrate-coated silver nanoparticles. Sci. Total Environ. 454–455, 119–131.
Liu, X., Jin, X., Cao, B., Tang, C.Y., 2014. Bactericidal activity of silver nanoparticles in environmentally relevant freshwater matrices: influences of organic matter and chelating agent. J. Environ. Chem. Eng. 2, 525–531.
Wagner, S., Gondikas, A., Neubauer, E., Hofmann, T., von der Kammer, F., 2014. Spot the difference: engineered and natural nanoparticles in the environment—release, behavior, and fate. Angew. Chem. Int. Ed. 53, 12398–12419.
SharMa, V.K., Siskova, K.M., Zboril, R., Gardea-Torresdey, J.L., 2014. Organic-coated silver nanoparticles in biological and environmental conditions: fate, stability and toxicity. Adv. Colloid Interface 204, 15–34.
Zhang, C., Lai, C., Zeng, G., Huang, D., Yang, C., Wang, Y., Zhou, Y., Cheng, M., 2006. Efficacy of carbonaceous nanocomposites for sorbing ionizable antibiotic sulfamethazine from aqueous solution. Water Res. 95, 103–112.
Zhang, Y., Chen, Y.S., Westerhoff, P., Crittenden, J., 2009. Impact of natural organic matter and divalent cations on the stability of aqueous nanoparticles. Water Res. 43, 4249–4257.
Chen, K.L., Mylon, S.E., Elimelech, M., 2007. Enhanced aggregation of alginate-coated iron oxide (hematite) nanoparticles in the presence of calcium, strontium, and barium cations. Langmuir 23, 5920–5928.
Zhang, H., Smith, J.A., Oyanedel-Craver, V., 2012. The effect of natural water conditions on the anti-bacterial performance and stability of silver nanoparticles capped with different polymers. Water Res. 46, 691–699.
Li, M., Pokhrel, S., Jin, X., Mädler, L., Damoiseaux, R., Hoek, E.M.V., 2011b. Stability, bioavailability, and bacterial toxicity of ZnO and iron-doped ZnO nanoparticles in aquatic media. Environ. Sci. Technol. 45, 755–761.
Kirk, T.K., Schultz, E., Connors, W.J., Lorenz, L.F., Zeikus, J.G., 1978. Influence of culture parameters on lignin metabolism by *Phanerochaete chrysosporium*. Arch. Microbiol. 117, 277–285.
Huang, Z., Chen, G., Zeng, G., Guo, Z., He, K., Hu, L., Wu, J., Zhang, L., Zhu, Y., Song, Z., 2017. Toxicity mechanisms and synergies of silver nanoparticles in 2,4-dichlorophenol degradation by *Phanerochaete chrysosporium*. J. Hazard. Mater. 321, 37–46.
Huang, Z., Xu, P., Chen, G., Zeng, G., Chen, A., Song, Z., He, K., Yuan, L., Li, H., Hu, L., 2018a. Silver ion-enhanced particle-specific cytotoxicity of silver nanoparticles and effect on the production of extracellular secretions of *Phanerochaete chrysosporium*. Chemosphere 196, 575–584.
Chen, A., Zeng, G., Chen, G., Liu, L., Shang, C., Hu, X., Lu, L., Chen, M., Zhou, Y., Zhang, Q., 2014. Plasma membrane behavior, oxidative damage, and defense mechanism in *Phanerochaete chrysosporium* under cadmium stress. Process Biochem. 49, 589–598.
Pokhrel, L.R., Andersen, C.P., Rygiewicz, P.T., Johnson, M.G., 2014b. Preferential interaction of Na^+ over K^+ with carboxylate-functionalized silver nanoparticles. Sci. Total Environ. 490, 11–18.
Zhao, C.M., Wang, W.X., 2012. Size-dependent uptake of silver nanoparticles in *Daphnia magna*. Environ. Sci. Technol. 46, 11345–11351.
Gliga, A.R., Skoglund, S., Wallinder, I.O., Fadeel, B., Karlsson, H.L., 2014. Size-dependent cytotoxicity of silver nanoparticles in human lung cells: the role of cellular uptake, agglomeration and Ag release. Part. Fibre Toxicol. 11, 11.
Osborne, O.J., Lin, S., Chang, C.H., Ji, Z., Yu, X., Wang, X., Lin, S., Xia, T., Nel, A.E., 2015. Organ-specific and size-dependent Ag nanoparticle toxicity in gills and intestines of adult zebrafish. ACS Nano 9, 9573–9584.
Chen, L.Q., Fang, L., Ling, J., Ding, C.Z., Kang, B., Huang, C.Z., 2015b. Nanotoxicity of silver nanoparticles to red blood cells: size dependent adsorption, uptake, and hemolytic activity. Chem. Res. Toxicol. 28, 501–509.
Liu, J., Legros, S., Von der Kammer, F., Hofmann, T., 2013. Natural organic matter concentration and hydrochemistry influence aggregation kinetics of functionalized engineered nanoparticles. Environ. Sci. Technol. 47, 4113–4120.
Sahalan, A.Z., Abd Aziz, A.H., Lian, H.H., Abd Ghani, M.K., 2013. Divalent cations (Mg^{2+}, Ca^{2+}) protect bacterial outer membrane damage by polymyxin B. Sains Malays. 42, 301–306.
Huynh, K.A., Chen, K.L., 2011. Aggregation kinetics of citrate and polyvinylpyrrolidone coated silver nanoparticles in monovalent and divalent electrolyte solutions. Environ. Sci. Technol. 45, 5564–5571.
Huang, Z.Z., He, K., Song, Z.X., Zeng, G.M., Chen, A.W., Yuan, L., Li, H., Hu, L., Guo, Z., Chen, G.Q., 2018b. Antioxidative response of *Phanerochaete chrysosporium* against silver nanoparticle-induced toxicity and its potential mechanism. Chemosphere 211, 573–583.
Tang, W.W., Zeng, G.M., Gong, J.L., Liang, J., Xu, P., Zhang, C., Huang, B.B., 2014. Impact of humic/fulvic acid on the removal of heavy metals from aqueous solutions using nanomaterials: a review. Sci. Total Environ. 468–469, 1014–1027.
Wan, J., Zeng, G., Huang, D., Hu, L., Xu, P., Huang, C., Deng, R., Xue, W., Lai, C., Zhou, C., Zheng, K., Ren, X., Gong, X., 2017. Rhamnolipid stabilized nano-chlorapatite: synthesis and enhancement effect on Pb- and Cd-immobilization in polluted sediment. J. Hazard. Mater. 343, 332–339.
Ren, X., Zeng, G., Tang, L., Wang, J., Wan, J., Liu, Y., Yu, J., Yi, H., Ye, S., Deng, R., 2018. Sorption, transport and biodegradation—an insight into bioavailability of persistent organic pollutants in soil. Sci. Total Environ. 610–611, 1154–1163.
Fabrega, J., Fawcett, S.R., Renshaw, J.C., Lead, J.R., 2009. Silver nanoparticle impact on bacterial growth: effect of pH, concentration, and organic matter. Environ. Sci. Technol. 43, 7285–7290.
Schaumann, G.E., Philippe, A., Bundschuh, M., Metreveli, G., Klitzke, S., Rakcheev, D., Grun, A., Kumahor, S.K., Kuhn, M., Baumann, T., Lang, F., Manz, W., Schulz, R., Vogel, H.J., 2015. Understanding the fate and biological effects of Ag- and TiO_2-nanoparticles in the environment: the quest for advanced analytics and interdisciplinary concepts. Sci. Total Environ. 535, 3–19.
Pandey, A.K., Pandey, S.D., Misra, V., 2000. Stability constants of metal–humic acid complexes and its role in environmental detoxification. Ecotoxicol. Environ. Saf. 47, 195–200.
Malekkhaiat, H.S., Malmsten, M., 2017. Membrane interactions and antimicrobial effects of inorganic nanoparticles. Adv. Colloid Interface Sci. 248, 105–128.
Huang, Z., Zeng, Z., Chen, A., Zeng, G., Xiao, R., Xu, P., He, K., Song, Z., Hu, L., Peng, M., Huang, T., Chen, G., 2018c. Differential behaviors of silver nanoparticles and silver ions towards cysteine: bioremediation and toxicity to *Phanerochaete chrysosporium*. Chemosphere 203, 199–208.
Xu, P., Zeng, G.M., Huang, D.L., Feng, C.L., Hu, S., Zhao, M.H., Lai, C., Wei, Z., Huang, C., Xie, G.X., Liu, Z.F., 2012a. Use of iron oxide nanomaterials in wastewater treatment: a review. Sci. Total Environ. 424, 1–10.
Xu, P., Zeng, G.M., Huang, D.L., Lai, C., Zhao, M.H., Wei, Z., Li, N.J., Huang, C., Xie, G.X., 2012b. Adsorption of Pb(II) by iron oxide nanoparticles immobilized *Phanerochaete chrysosporium*: equilibrium, kinetic, thermodynamic and mechanisms analysis. Chem. Eng. J. 203, 423–431.